Stochastic Response of Jacket Supported Offshore Wind Turbines for Varying Soil Parameters

Abhinav K A[a], Nilanjan Saha[a,*]

[a] *Dept. of Ocean Engineering, Indian Institute of Technology - Madras, Chennai, India*

Abstract

Wind turbines on jackets are being increasingly installed offshore. This paper attempts to investigate the effect of soil-structure interaction (SSI) on a jacket-offshore wind turbine (OWT) in a water depth of 70 m using JONSWAP spectrum. Stochastic responses of the OWT under varying soil profiles and met-ocean conditions are studied, by coupling the aerodynamic and hydrodynamic forces. From stochastic time domain response analyses, the SSI is observed to have significant influence in soft clay and layered soils at and above rated wind speeds whereas the dense sand have negligible influence.

Keywords: Jacket, Offshore wind turbines, Soil-structure interaction, Stochastic response analysis

2010 MSC: 00-01, 99-00

*Corresponding author

Email address: nilanjan@iitm.ac.in (Nilanjan Saha)

1. Introduction

Wind turbines are increasingly being installed in offshore deeper waters due to higher wind speeds and lesser visual impact. Additionally, lower turbulence, ease of transportation and abundance of available sites make offshore wind energy an attractive proposition [1]. The design of substructures and foundations for offshore wind turbines (OWTs) are borrowed from the prevailing concepts in the offshore oil and gas industry. However, a proper coupled dynamic analysis is necessary to predict the response and comprehend the modes of failure. As unlike in the case of oil platforms, OWTs may be more flexible and are subjected to high lateral loads, from combined wind, waves and currents, to the tune of 50 to 150% of the vertical loading [2]. This calls for a detailed analysis of the different loading effects for the OWT structures [3].

One major factor that determines the substructure for offshore wind turbines is the water depth at the installation site. Monopiles till now have been widely used as a support for OWTs in shallow waters (less than 25 m of water depth) and over 75% of the installed OWTs in Europe are on monopiles [4]. However, for deeper water depths within $40 - 100$ m, jackets are usually preferred ones as they are hydrodynamically transparent to wave forces [5]. A detailed review of various substructure concepts of OWTs has been discussed in [6]. The use of jackets as support structures for OWTs is gaining prominence (*e.g.*, the Alpha Ventus and the Beatrice Demonstrator [7]). Recent studies have also analyzed the response of jacket supported OWTs under the aerodynamic and hydrodynamic loads [8, 9, 10, 11]. However, the above studies do not consider soil-structure interaction and assume the jackets are considered to be fixed at the mudline. This exclusion of soil in analysis is a reasonable assumption for 'stiff/rigid' soils whereas the soil effects becomes more important when OWTs are installed in 'softer' marine soils [12] or a combination of loads acts on the structure. Therefore to obtain the response of OWT installations in softer soils, a combined analysis under different loads is necessary to avoid resonance effects.

Based on the experiences in the German industry, a comprehensive review of the prevalent methodologies for the design of the OWT foundation was reported by [2]. The limitations of the $p-y$ method in offshore design standards [13, 14] vis-à-vis offshore industry practices have been reviewed by [15] and it was concluded that a proper finite element analysis for addressing non-linearities in soil-behaviour is necessary. A scaled model of 3 MW Vestas V90 OWT was experimentally studied to illustrate the effects in kaolin clay under cyclic loading by [16]. They reported that shear strain of the soil changes considerably and therefore its has a considerable effect on the natural frequency variation. A guideline on the choice of monopile diameters have also been proposed. Another work using shake table experiments to investigate the liquefaction effects on natural frequency and damping on pile supported structures was studied by [17]. They found that natural frequencies changed considerably due to seismic liquefaction. The long term effects of cyclic loading on piles supporting OWT was evaluated by [18] and they concluded that cyclic loading increased stiffness contrary to degradation. To study the effect of the soil flexibility of wind turbines, an experimental model was developed by [19]. The results are then validated by modelling the wind turbine as an Euler Bernoulli beam using a finite element framework. The complete wind turbine is modelled as a beam with one end being supported by translational and rotational spring (soil model) while the other end of the beam having a lumped mass (rotor-nacelle-assembly model). These authors also derived an expression in another work [20] to obtain the natural frequency of the wind turbine structure. This closed-form expression included the properties of soil as parameters. Studies on effect of shear strain on natural frequencies were experimentally analysed for three different footings - symmetric tetrapod, monopile and asymmetric tripod on suction caissons by [21, 22]. All the above studies are using monopiles to study effect on natural frequencies and the OWT response did not consider the combined effect of aerodynamic and hydrodynamic loads along with the soil.

There are also few attempts in literature, wherein, the effect of wind and wave loads on the response of OWTs on framed structures (*i.e.*, jackets) along with soil effects have been investigated. The effects of soil-structure interaction ('hard' soil *i.e.*, interface friction angle greater than 35°) using fixed-base method, the $p - y$ method and the pile group effect was studied by [23] to understand the performance of braces in jacket OWTs. Seismic studies on jacket OWTs have been conducted by [24] to understand their effects on overall performance during the earthquakes. There also exist some studies only for jacket structures without the wind turbine. One example is the parametric study on the response of jacket structure subjected to transient loading under extreme waves by [25]. Though there have been studies where the loading effects of OWT have been studied separately, however a combined aerodynamic, hydrodynamic and geotechnical analysis for OWTs is necessary. As offshore farms can be located where varying soil conditions are present, a parametric analysis under operational and parked conditions using various soil parameters is also important.

In this paper, the jacket supported NREL 5 MW OWT [26] response for various soil profiles is analysed. The OWT response (tower top displacement and forces at the jacket-base) are studied keeping into mind that the serviceability limit state criteria (displacements) is satisfied. Each soil profile is studied under different sea-state condition (wind speed, significant wave height and peak spectral period) as per JONSWAP spectrum. The sea-states are chosen such that three are in operational regime (below rated, at rated and above rated wind speeds) while one is in idling regime (beyond cut-out wind speed). Soil properties along the pile are modelled using the *p-y, t-z* and *Q-z* curves as recommended by modern design standards [13, 14]. In this work, these curves are represented through nonlinear springs along the length of the pile. The hydrodynamic loads are modelled using USFOS [27] whereas the aerodynamic loads are obtained using the aerodynamic code FAST [28]. Since the loading becomes stochastic/random due to turbulent wind conditions and irregular (JONSWAP spectrum) waves, the OWT response has to be handled in a random framework. Therefore, 25 Monte Carlo Simulations are carried out in time domain for each case and the response obtained is through ensemble averaging. The paper now runs with additional four sections. The structural, geotechnical and

NREL 5MW OWT [26] models used in the study are detailed in section §2. The section also details the numerical methods. Theoretical background for the combination of aerodynamic and hydrodynamic load calculations is briefly explained in section §3. Section §4 focuses on the research findings of the present study and the paper concludes with section §5. Note that in the paper, the term 'foundation' refers to the piles embedded in the soil, where as the 'substructure' stands for the braced jacket, extending from the transition piece to the pile heads.

2. Model Specification

2.1. NREL 5MW Offshore Wind Turbine

The NREL 5MW OWT, conceptualized on the REpower 5MW turbine [26], is considered for the present work. The wind turbine (rotor-nacelle assembly) is placed on a tapering circular steel tower (70 m long) placed on a jacket structure. The tower top (or the yaw-bearing), is located at a height of 88.15 m above the mean sea level (MSL) and the tower outer diameter varies from 5.6 m at the base to 4 m at the top. A transition piece joins the tower with the jacket and this transition piece (of length 4 m) is modelled by means of simple rectangular beam elements.The steel transition piece has a mass of 666 t with density 15.14×10^3 kg/m^3 so as to compensate for not including bolts, flanges and welds in the numerical model. The tower and turbine is modelled using the information available in [29]. The tower model details are reproduced in Table 1. This OWT has been widely used as a benchmark for wind energy studies and its defining features are given in Table 2. It is a 3-bladed, variable speed, pitch controlled turbine with an upwind rotor configuration and is a representative model of the multi-megawatt OWTs.

2.2. Jacket Substructure

Jackets are three dimensional space frame structures widely used as offshore oil platforms. The present model is a four-legged structure that is supported

Table 1: OWT tower dimensions [29]

Design level (m).	Outer diameter (m)	Thickness (mm)
88.15	4.000	30
83.15	4.118	30
74.15	4.329	20
64.15	4.565	22
54.15	4.800	24
42.15	5.082	28
32.15	5.318	30
21.15	5.577	32
20.15	5.600	32

Table 2: Properties of NREL 5MW OWT [26]

Parameter	Value
Power rating	5 MW
Rotor orientation	Upwind
Rotor, Hub diameter	126 m, 3 m
Rated rotor speed	12.1 rpm
Cut-in wind speed	3 m/s
Rated wind speed	11.4 m/s
Cut-out wind speed	25 m/s
Rotor-nacelle-assembly mass	$350,000$kg

through pile foundations. The water depth at the site is 70 m. The jacket structure extends 20 m above the mean sea level (MSL). The jacket has a footprint of 32 m $\times$ 32 m at the mudline. Five bays of $X-$bracings interconnect the main tubular legs while two horizontal $X-$bracings are placed at 2.5 m and 50 m height above the mudline. Fewer horizontal bracings are requierd as the top deck and foundation also provide sufficient horizontal rigidity to the structure. The piles are terminated at a depth of 45 m below the mudline and are of 1.8 m in diameter and of wall thickness 4 cm. The jacket is developed using two-noded beam elements.

The finite element code USFOS [27], is used to model the jacket. USFOS is a well-known software in offshore industry for non-linear analysis of space-frame structures which has the ability to model hydrodynamic loading as well as geotechnical effects. USFOS makes use of the Idealized Structural Unit Method (ISUM) [30], for discretization of the structure, wherein one actual element in the jacket is represented by one finite element [31]. In other words, by ISUM one discretizes the structure into actual physical units thereby by passing the requirement of choosing element and mesh sizes as in traditional FEM. The motivation behind using the ISUM is to achieve savings in computational and data costs, by reducing the number of elements and degrees of freedom [32]. ISUM has therefore found numerous applications in ship structures, offshore structures (*e.g.*, jackets) as well as bridge metal girders as an alternative to finite element formulation without compromising on the accuracy of the results [30]. The formulation is based on Green strain, which is able to capture large displacement effects and the lateral deflection-axial strain coupling. Using the Green strain formulation, one can therefore account for column bucking and membrane effects in tubular members in jackets. The large displacements are taken care by updating the system information at every increment/step using an updated Lagrangian formulation. By this updated formulation, the loads are incrementally increased at every time step and the incremental load is reversed the moment a global instability occurs. In each incremental step, the updated coordinates of the system along with the information of the immediate previous

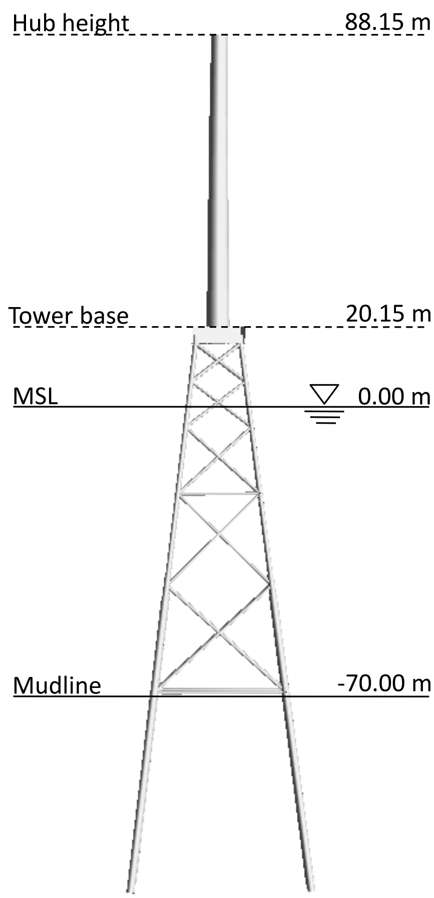

Figure 1: FE model of jacket supporting OWT

step is used to perform the analysis. The representative model of the jacket is shown in Figure 1. The effect soil properties on the global response are illustrated using load effects *i.e.*, top tower displacement or pile displacement. The material properties of the jacket are shown in Table 3.

2.3. Soil Model

Usually the offshore structures are bottom supported by piles which fail either by pull-out in tension (due to cyclic loading) or via punch-through in compression due to large axial loads. Now for OWTs where the piles experience large lateral loads, either they fail due to rotation as rigid bodies or due to

Table 3: Material properties of the jacket

Part	Elastic modulus (N/m^2)	Yield stress (N/m^2)	Density (N/m^3)
Jacket	2.10×10^{11}	4.20×10^{8}	7.85×10^{3}
Transition piece	2.10×10^{11}	4.20×10^{11}	15.14×10^{3}
Tower	2.10×10^{11}	4.20×10^{11}	8.50×10^{3}
Piles	2.10×10^{11}	4.20×10^{8}	7.85×10^{3}

the failure of soil-wedge supporting the pile (*i.e.*, thus experiencing toe-kick). Also the lateral loads may cause failure due to bending in flexible piles (soft soil scenarios) or due to large slenderness ratios. The soil structure interaction (SSI) can be modelled by means of independent nonlinear springs located along the length of the pile or by using finite element continuum models. These non-linear load displacement curve can be modelled either by piece-wise linear springs or by plastic hinge concepts [33]. Studies have shown that an offshore structure can fail due to inappropriate load distribution curves along the pile [34]. Therefore, choosing an appropriate pile-soil model is important to comprehend failure. For example, if one uses a linear spring model for pile foundation, then one may do an gross overestimation of the system capacity in some cases [35].

As per the offshore standards [13, 14], the non-linear springs are to be discretely placed along the length of the pile in order to capture the effect of soil structure interaction. These $p - y$ curves are widely used for pile design in offshore energy sector [36] and one obtains the lateral spring stiffness from the gradient of the soil resistance (p) versus deflection (y) curve. Similar the $t - z$ and $Q - z$ curves are used for estimation of skin friction resistance in the vertical direction and the tip bearing resistance. The concept of $p - y$ curves has been extensively examined in [37] are briefly described below.

$p - y$ curves for sand are defined by [13] as follows:

$$p = Ap_u tanh\left(\frac{kx}{Ap_u} y\right) \tag{1}$$

where the value of A depends on the nature of the loading. A_s and A_c are used for static and cyclic loading, respectively.

$$\begin{aligned} A_s &= \left(3.0 - 0.8\frac{x}{D}\right) \geq 0.9 \\ A_c &= 0.9 \end{aligned} \tag{2}$$

In the above equations, p_u is the ultimate lateral bearing capacity at a depth x and k is the initial modulus of subgrade reaction, obtained from [13], as a function of ϕ, the angle of internal friction. p_u values are computed for both shallow and deeper depths, as p_{us} and p_{ud} respectively and the lower value is used as the ultimate lateral bearing capacity for sand.

For soft clay below the water table, [13] derives $p-y$ curves on the basis of [38]. Initially, the ultimate soil resistance per unit length of the pile, p_{ult}, is obtained as the minimum of the two values in equation 3.

$$\begin{aligned} p_{ult} &= \left(3 + \frac{\gamma}{c_u}x + \frac{J}{d}x\right) c_u d \\ p_{ult} &= 9c_u d \end{aligned} \tag{3}$$

where γ is the effective unit weight of soil in, d is the pile diameter, c_u is the undrained shear strength at a depth x and J is an experimental coefficient with values of 0.5 and 0.25 for soft and medium clays, respectively. The $p-y$ curves are now described using the relationship given in equation 4.

$$\frac{p}{p_{ult}} = 0.5\left(\frac{y}{y_{50}}\right)^{\frac{1}{3}} \tag{4}$$

p and y are the soil resistance per unit length of the pile and the lateral deflection, respectively. y_{50} is the deflection at half the ultimate soil resistance and is obtained as follows:

$$y_{50} = 2.5\epsilon_{50}d \tag{5}$$

ϵ_{50} is the strain at half the maximum stress on undrained compression tests of undisturbed soil samples [13]. Above $y = 8y_{50}$, p has a constant value.

In this work, USFOS is used to perform the geotechnical analysis which also uses the API code for obtaining the resistance curves. In USFOS, a node (finite element) is generated along the pile at the center of each soil layer along its length. The pile is modelled as a nonlinear beam elements joining two consecutive nodes. The soil is modelled using spring-to-ground elements attached to each of the corresponding node. Two nonlinear soil springs representing soil properties - lateral resistance and skin friction- are attached to each node. Depending on the required accuracy, the node to node distance can be decreased. The piles are oriented in the same angle as the main legs of the jacket extending to a depth of 45 m from the mudline.

A convergence study with respect to the centre-to-centre spacing of soil springs attached to the pile, is essential to determine the optimum value of spacing. A sample pile with similar characteristics to the ones supporting the jacket OWT (*i.e.* 1.8 m diameter and 45 m depth), in dense sand, was analyzed by reducing the spacing between soil-springs from 8 m through to 1 m. A lateral load of 2 MN was applied at the pile head. Figure 2 shows the variation in the lateral displacement of the pile head, with decreasing centre-to-centre spacing between the soil springs. The spacing between springs attains an optimal value at 2 m, as seen in the figure. Henceforth, the spacing is fixed at 2 m centre to centre for all analyses, except for specific layers in the layered soil, where thickness is less than 2 m. Soil springs are placed at the centre of such layers.

2.4. Validation of Numerical Model

The suitability of USFOS to model the jacket supported OWT problem was checked for, through validation tests. A model of the OC4 jacket supporting the NREL 5 MW OWT was subjected to natural frequency and displacement tests in USFOS and the values were compared with that of [39], who made use of SubDyn [40] in their study. In the displacement analysis, lateral loads of varying magnitude were applied at the tower top and the corresponding displacements at the tower top and tower base were determined. As shown in Table 4 and Table 5, USFOS was able to predict the response of the OC4 jacket, with a

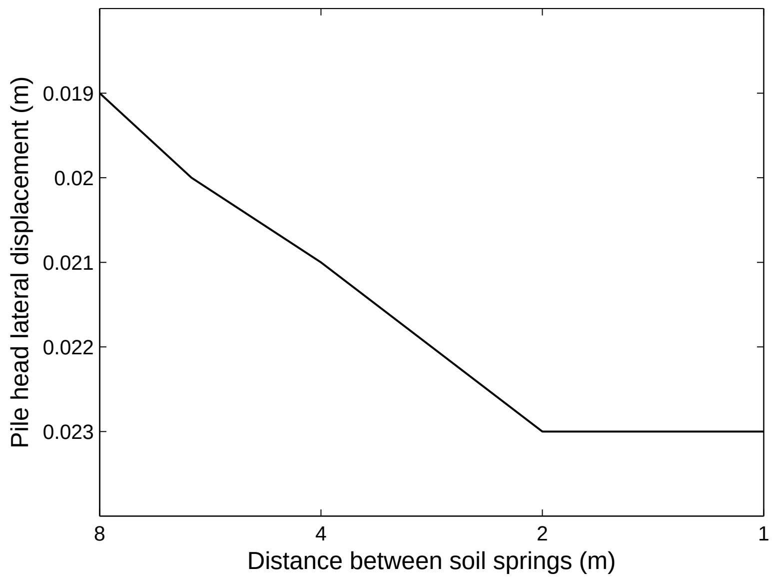

Figure 2: Convergence of soil spring density

reasonable amount of accuracy.

3. Loads on Offshore Wind Turbine

An OWT is subjected to the action of both aerodynamic and hydrodynamic loads. Here, the wind and waves are considered to be collinear *i.e.*, no effect of directionality is considered. The present study ignores current loads and loads arising from the wind shear effect on the tubular tower. Further, the effect of

Table 4: Natural frequencies of OC4 jacket in Hz

Mode no.	Song *et al.* [39]	USFOS
1	0.319	0.314
2	0.319	0.314
3	1.194	1.170
4	1.194	1.170

Table 5: Analysis of OC4 jacket

Thrust at tower top (kN)	Song *et al.* [39]	USFOS
	Displacement at tower top (m)	
2000	1.21	1.26
4000	2.42	2.52
	Displacement at tower base (m)	
2000	0.14	0.14
4000	0.28	0.28

marine growth along the jacket members is not considered.

3.1. Aerodynamic Loads

The time series of aerodynamic loads acting at the hub of the NREL 5MW OWT are realized using NREL's FAST [28] program. FAST acts on three dimensional full field wind files generated by TurbSim [41], which is a stochastic wind simulator and makes use of the modified blade element momentum theory [42] by considering wake effects to compute the aerodynamic loads on the hub.

The wind velocity increases with height from the ground, due to the waning influence of the earth's friction - a phenomenon called wind shear [43]. In the present work, the wind velocity profile is predicted by means of a logarithmic law [14, 44], given by equation (6):

$$\frac{U_z}{U_{z_r}} = \frac{\ln\left(\frac{z}{z_0}\right)}{\ln\left(\frac{z}{z_r}\right)} \tag{6}$$

Here, U_z is the mean wind speed at a height z above the mean sea level, U_{z_r} is the mean wind speed at a reference height z_r and z_0 is a surface roughness length parameter. The actual wind speed at any point may be represented as the sum of a mean wind speed and a fluctuating component arising from turbulence. Turbulence is defined as the random perturbations imposed on the mean wind speed, in three directions, during the transformation of the kinetic energy of the wind to thermal energy [44]. Turbulence is quantified in terms of turbulence intensity, which is the ratio of the standard deviation of wind speed to the mean wind speed. Normal Turbulence Model, wherein the turbulence intensity decreases monotonically with increasing wind speed, is considered in the study. The frequency content of the wind velocity is described using the Kaimal spectrum [45], stated in equation (7):

$$S(f) = \frac{4{\sigma_v}^2 L_k/u_h}{(1 + 6fL_k/u_h)^{5/3}} \tag{7}$$

where f is the cyclic frequency, L_k is an integral length scale parameter, u_h is the mean wind speed and σ_v is its standard deviation. Using the above stated parameters, the stochastic wind simulator, TurbSim [41] generates time series of 3-component wind vectors over a rectangular grid, encompassing the turbine rotor. The time series are now marched at the mean wind speed, in the mean wind direction. This may be visualized as a "full-field" of three-dimensional space, filled with instantaneous wind speeds [46]. The AeroDyn [42] component of FAST determines the velocity components on the blade element locations, through linear interpolation on the full-field wind data. The aerodynamic loads acting on the blades and the hub of the OWT are now computed using the blade element momentum (BEM) theory [47]. The BEM theory is composed of two sub-theories: the blade element theory and the momentum theory. According to the blade element theory, the total aerodynamic force on the blade can be determined as the sum of the forces acting on the discrete blade elements along its span. The momentum theory makes use of the conservation of momentum to determine the forces and flow conditions on a OWT blade.

3.2. Hydrodynamic Loads

Being hydrodynamically transparent structure, the wave forces on the jacket can be obtained using Morison's equation. Both FAST and USFOS computes wave loads on the jacket, using Morison's equation [48]. Using this equation, one computes the wave loads on fixed cylindrical structures as the sum of inertia and nonlinear drag forces. Accordingly, the force per unit length of a cylinder is given by equation (8):

$$F = \rho C_M \frac{\pi D^2}{4}\dot{u} + \frac{1}{2}\rho C_D |u|\ u \tag{8}$$

Here, F stands for the horizontal force on the cylinder per unit length, D represents the diameter of the cylinder and u stands for the relative water particle velocity in the horizontal direction. C_M and C_D are the empirical hydrodynamic coefficients for inertia and drag, respectively and ρ is the density of sea water. The upper dot stands for time derivative.

Ocean waves are characterized by their inherent irregularity. Irregular sea elevations may be assumed to be Gaussian-distributed zero-mean stationary stochastic processes [49]. In the present study, the time histories of irregular waves are generated from the JONSWAP spectrum [50]. The JONSWAP spectrum is valid for limited fetch conditions and is extensively used in the offshore industry. A constant area method is used for discretization of the spectrum - here, the spectrum is split into components of equal area (or energy). Each wave component is associated with a harmonic wave of given amplitude, angular frequency and random phase angle. The wave surface elevation is now realized through the superposition of all harmonic wave components. This method is called as the Deterministic Spectral Amplitude (DSA) model and the wave surface elevation, $\eta(t)$ is represented using Rice's equations [51] [52] as follows:

$$\eta(t) = \sum_{i=1}^{N} A_i \cos(\omega_i t - \psi_i) \tag{9}$$

$$A_i = \sqrt{2S(\omega_i)\Delta\omega_i} \tag{10}$$

Here, A_i refers to the deterministic wave amplitude, ω is the energy spectrum under consideration, $\Delta\omega$ is the discretization frequency and ψ_i is the random phase added to preserve the randomness of the time series. The spectrum is discretized into 300 frequencies for generation of time series of sea surface elevation.

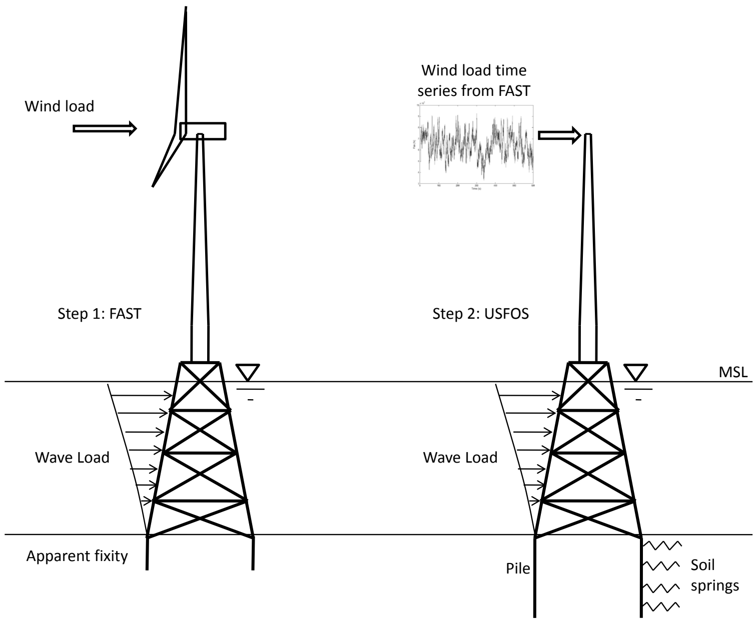

Figure 3: Combining loads for OWT analysis

3.3. Coupling of Loads

The program FAST is capable of coupled aerodynamic-hydrodynamic analyses, but lacks geotechnical capabilities. On the other hand, USFOS can simulate responses arising from hydrodynamic-geotechnical coupling. Thus, there arises a need to combine the load effects of these two computer programs to realize the response of a jacket supported OWT under wind and wave loading, in the presence of soil. Wind-wave analyses for fixed OWTs can produce conservative estimates of structural response, when the natural period of the jacket is lower than the period of the forcing waves [53, 54]. The present work makes use of a coupling approach for wind and wave loads, which involves a two-step procedure, as illustrated in Figure 3: a) derivation of the time-series of wind loads acting at the OWT hub, using FAST and b) subsequently the analyses in USFOS by including the wind loads from FAST.

In the first step, the jacket model is incorporated into FAST, for coupled

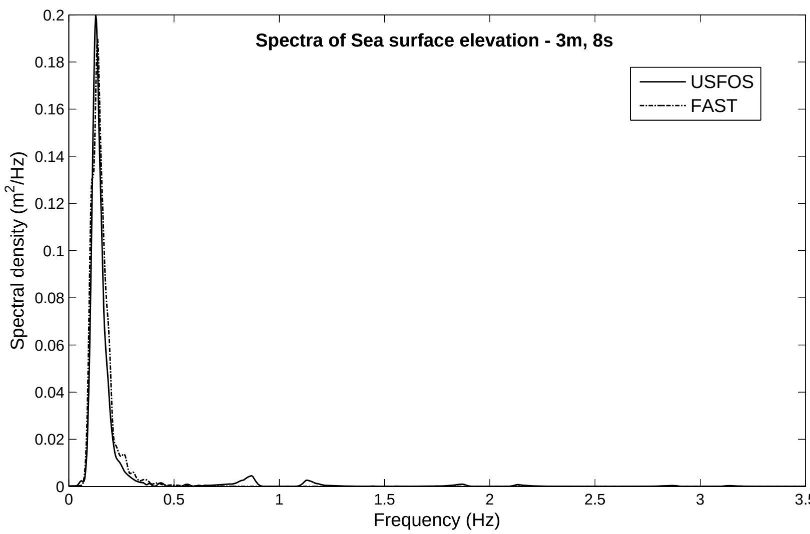

Figure 4: Spectra of sea surface elevation

aerodynamic-hydrodynamic analysis. The jacket is fixed at the mudline and the effect of SSI is mimicked by means of an apparent fixity model, which approximates the pile-soil stiffness by means of a fictitious cantilever extending beneath the mudline. This fictitious cantilever would produce mudline deflection and rotation identical to that by the actual pile-soil system, under similar loading conditions. Derivation of apparent fixity has been extensively discussed in literature [55, 56]. In the second step, coupled hydrodynamic-geotechnical analyses are performed in USFOS, in the presence of the time-series of hub-height wind loads exported from FAST. For such a coupled approach, it is essential that the wave generation capabilities of the two programs should be similar [57]. As observed in Figure 4, showing the spectra of sea surface elevation for a sample sea state characterized by a significant wave height of 3 m and peak spectral period of 8 s, FAST and USFOS have identical programs for the generation of wave loading.

3.4. Pushover Analysis

Pushover analysis is used as a tool to determine the ultimate capacity of structures under lateral loads [58], such as waves and earthquakes. Pushover analysis is conducted in two stages [33]: initially, the permanent loads on the structure (self weight) are incremented to a value of unity. In the second stage, the environmental load is gradually increased till eventual collapse of the structure. The resultant load-displacement curve is indicative of the behavior of the structure during and beyond the collapse.

3.5. Dynamic Analysis

The dynamic model of an offshore jacket subjected to environmental loading may be represented as follows:

$$[M]\ddot{X} + [C]\dot{X} + [K]X = \{F(t)\} \tag{11}$$

In equation (11), $[M]$, $[C]$ and $[K]$ represent the mass, damping and stiffness matrices, respectively. $\{F(t)\}$ is the vector of external forces on the system. X stands for the vector of displacements and its time derivatives (velocities and accelerations) are indicated by means of dots above the symbols. The present work makes use of the Hilbert-Hughes-Taylor-α method [59] for numerical time integration. This method is a variation of the Newmark-β method (where, $\alpha = 0$). Here, the parameter α represents the time averaging of damping, stiffness and load terms [31]. Artificial damping is induced in the higher order vibration modes, without compromising the accuracy.

4. Modelling Parameters

Four different wind speeds and their corresponding wave conditions (significant wave height and peak spectral method) are considered for the analysis. The first three wind speeds are in the operational regime (at the rated wind speed of wind turbine, and additionally above and below the rated wind speeds) of the NREL 5 MW OWT, whereas the remaining one is representative of an extreme scenario (*i.e.*, idling condition of turbine). Under extreme wind speeds,

Table 6: Load cases for OWT analysis

Load case	V_w (m/s)	H_s (m)	T_p (s)	TI	Remarks
1	6.0	2.2	9.8	0.20	Below rated wind speed
2	11.4	3.1	10.1	0.15	At rated wind speed
3	24.0	5.7	11.2	0.12	Above rated wind speed
4	45.0	11.2	13.5	0.10	Extreme wind speed

the OWT blades are in a parked condition and there is no power production. Wind and waves are correlated and their simultaneous occurrence is predicted on the basis of JONSWAP spectrum [60]. The joint density function for wind and wind generated waves has been further elucidated by [61]. The chosen met-ocean states used in the study are specified in Table 6. Here, V_w refers to the 10-minute mean wind speed at the hub-height and TI represents the turbulence intensity. Each sea-state is denoted by a significant wave height (H_s) - peak spectral period (T_p) pair. In order not to write the details (quartet V_w, TI, H_s, T_p) of sea states while representing results, it is termed as four different load cases as mentioned in Table 6. The values for those reported in table are obtained using [60, 61].

Each sea state (V_w, H_s, T_p) response of the OWT is studied under three different soil compositions - uniform sand, layered soil and soft to medium stiff clay [62] (henceforth referred to as soft clay) profiles. The layered soil profile is composed of interspersed layers of sand and clay and the clay profile has layers of varying stiffness. The layered soil profiles are representative of existing soil conditions at sites off the eastern Indian coasts. The soil properties are defined in Tables 7, 8 and 9. Here, γ' refers to the effective unit weight of soil, Φ, to the angle of internal friction and S_u stands for undrained shear strength. ϵ_{50} is the strain at 50% failure stress, in percentage and K stands for the modulus of subgrade reaction. The classification of sands is based on the values given in [63].

The wave loading is random due to irregular (Gaussian) nature which is

Table 7: Sandy soil profiles

Depth (m)	Type	γ' (kN/m^3)	Φ ($^\circ$)	K (MN/m^3)
Loose sand				
0.0$\rightarrow$	sand	10	28	2.9
Medium dense sand				
0.0$\rightarrow$	sand	10	33	16.3
Dense sand				
0.0$\rightarrow$	sand	10	37.5	30.8

Table 8: Layered soil profile

Depth (m)	Type	γ' (kN/m^3)	Φ ($^\circ$)	S_u (kPa)	ϵ_{50}	K (MN/m^3)
0.0 - 1.5	sand	8	20			5.5
1.5 - 5.2	clay	8		20	1.5	
5.2 - 6.6	sand	8.5	20			5.5
6.6 - 8.8	clay	8.5		20	1.5	
8.8 - 11.7	sand	9	25			5.5
11.7 - 13.1	sand	9	30			16.6
13.1 - 15.6	clay	8.5		35	1.5	
15.6 - 16.7	sand	9	25			5.5
16.7 - 37.0	sand	9	30			16.6
37.0 - 50.0	clay	8.5		110	0.5	

Table 9: Soft clay soil profile

Depth (m)	Type	γ' (kN/m^3)	S_u (kPa)	ϵ_{50}
0.0 - 14.6	clay	5	2 - 14	2
14.6 - 27.1	clay	8	29 - 72	2
27.1 - 50.0	clay	8.5	72 - 77	2

obtained from the wave elevation equation (9). The turbulence intensity also causes randomness in the wind speeds and thereby aerodynamic loads. Therefore, the average response needs to be obtained for ensemble of realizations or Monte Carlo simulations. Pseudo-random number generators are generated to realize time series of wind and wave loading. The use of this approach ensures the reproduction of the same time series, by using the same random seed [9]. Variation in the random seed results in the realizations of different time series for the given set of wind (or wave) parameters, which causes epistemic uncertainties during load and response computations [64]. Such uncertainty may be eliminated by increasing the sample size, *i.e.*, by performing a large number of simulations with varying random seeds. The present study makes use of 25 Monte Carlo simulations of wind and wave time series for each load case. Each simulation is performed for a duration of 600 s as the wind speed averages are usually range for 10−min. In order to show the number of samples necessary to obtain reasonable ensemble averages, a representative figure for statistics of tower top deflection response is shown in Figure 5. The figure shows that with increase in number of ensemble size of Monte Carlo samples the ensemble averaged statistics converges. Therefore, the ensemble size is chosen as 25 for future calculations. One should note that due to inhomogeneity of the soils and non-linear interaction due to pile-soil springs, the skewness and kurtosis changes considerably with respect to fixed base. One of the reasons that non-Gaussianity effect is changed is due to the additional flexibility of the soils which may lead to change of natural frequency.

5. Numerical Illustrations

This section deals with the variation of structural responses on the jacket supported OWT arising from different soil and load conditions. The lateral displacement plots are shown with respect to the center line (vertical axis) of the jacket which is shown through Figure 6. It shows the vertical levels at where the response is measured along the jacket and tower. Also the the plan figure

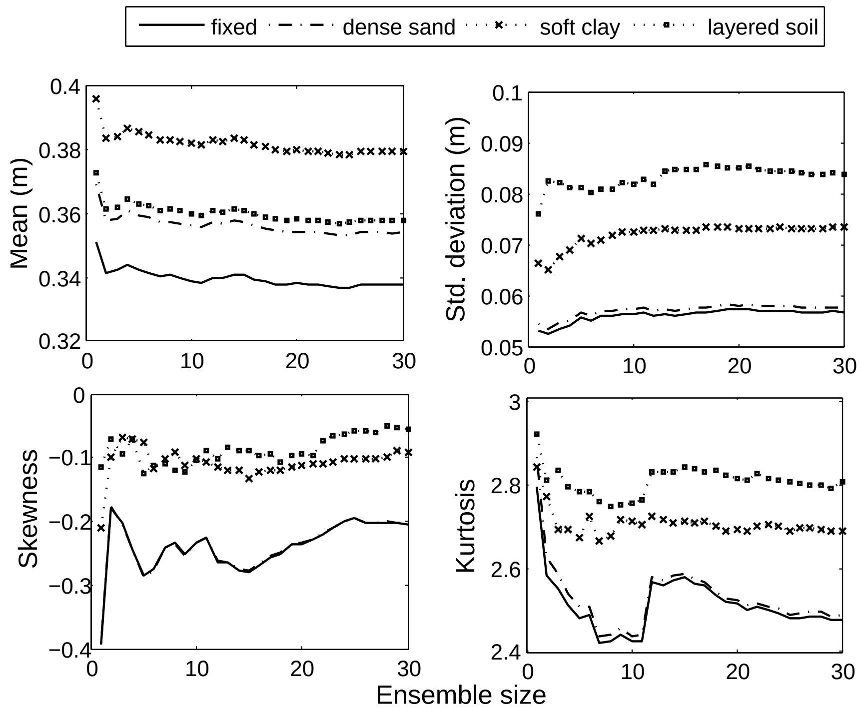

Figure 5: Convergence of statistical parameters for tower top deflection with increasing seeds

shows the exact location where the response is measured. The plots use an exaggerated horizontal scale for a better visibility of the response.

5.1. Variation of response with angle of internal friction

Three types of sandy soil, differentiated on the basis of the angle of internal friction are considered - dense, medium dense and loose sands. In USFOS, soil stiffness is obtained as the initial slope of the $p - y$ curves. For sands, the initial slope of the $p - y$ curves are developed as per the API recommendations and they are dependent on the angle of internal friction. Thus, an increase in the angle of internal friction gives stiffer soils with greater soil-pile resistance accompanied by a reduction in the response to loading. It may also be noted that the unit weight of the soil has a minimal bearing on the initial slope of the $p - y$ curves.

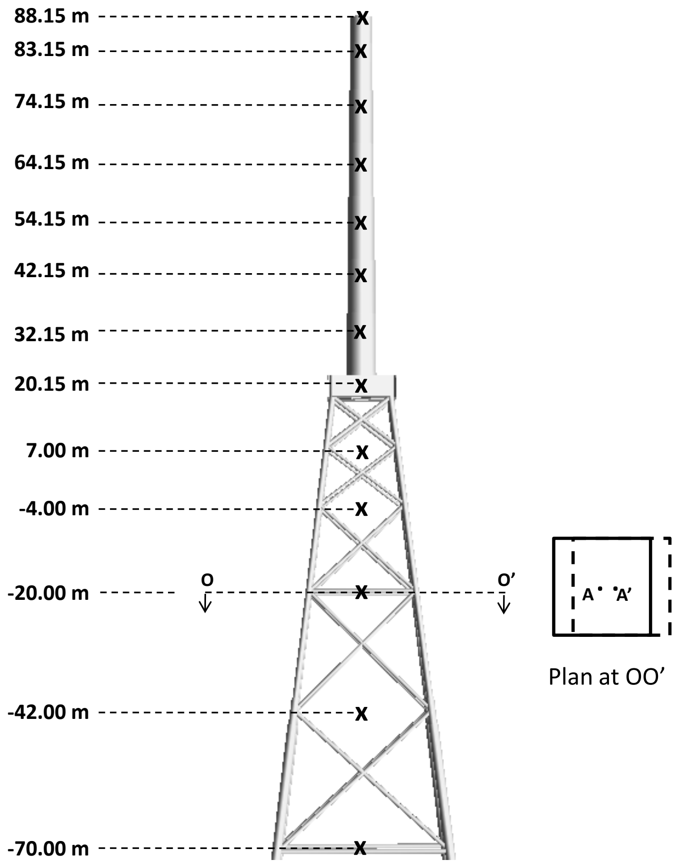

Figure 6: The locations at which responses are being measured

Table 10: Pile top displacements in sand

Type of sand	Pile top displacement (cm)
Dense	0.1
Medium dense	0.3
Loose	1.0

Wind and wave conditions corresponding to the rated wind speed of 11.4 m/s (Load Case 2, cf. Table 6) are imposed on the structure. The rated wind speed corresponds to the first time maximum power output is achieved by the turbine [44]. Figure 7 shows the ensemble averaged maxima of the lateral response of the jacket supporting the NREL 5 MW OWT in sandy soils of varying stiffness. Though the stiffness changes across the three sandy soil profiles, a significant variation in the lateral displacement of the structure, along the tower, is not visible. However, below the MSL, there is a marginal increase in response with reduction in stiffness of the sandy soil (up to ten times for loose sand). This can be observed from the maximum pile top displacement values at the mudline, shown in Table 10. As the sandy profile, do not affect the responses, the further analysis considers in the study the dense sand profile only.

5.2. Influence of SSI

As mentioned in the introduction, OWTs supported on jackets have often been studied as fixed bottom structures and the contribution of SSI is ignored. Under such an assumption, the legs of the substructure are pinned to the mudline. In the present section, the ensemble averaged maxima response of the OWT structure at the rated wind speed is investigated by pinning the legs to the mudline. This is compared with the response obtained by including the soil component, in Figure 8. As opposed to a fixed based model, introduction of soil induces a certain degree of flexibility into the system, thereby resulting in an escalation of response, the magnitude of which, is dependent on the stiffness of the soil.

As observed from Figure 8, the stiffer dense sand has a lateral response

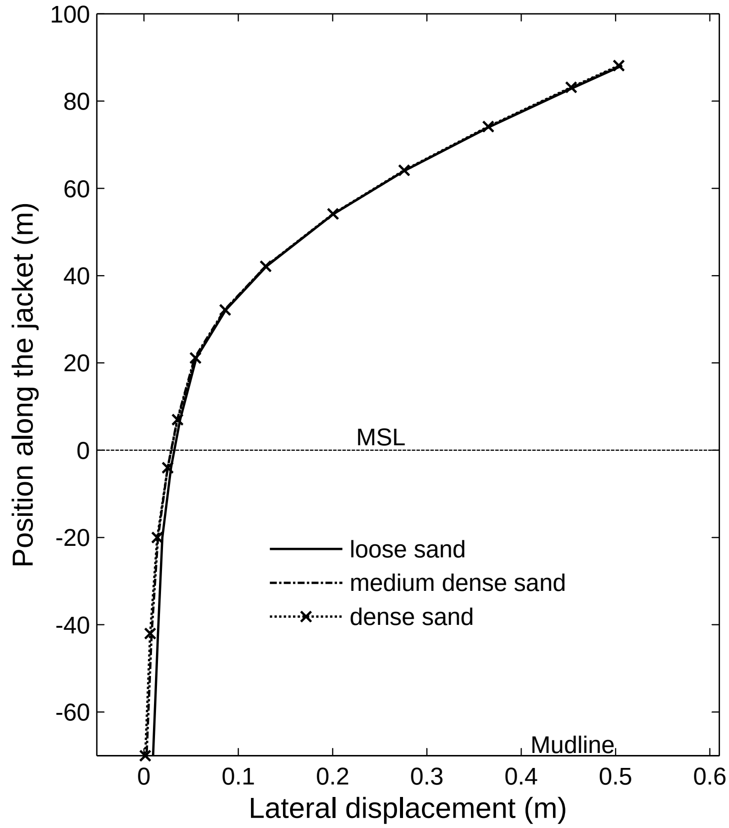

Figure 7: Variation of ensemble-average of maxima of lateral displacement for various types of sand

marginally greater than that of the fixed OWT. However, offshore wind farms may not always be sited on such uniform, ideal soil profiles and this necessitates the analysis of OWTs using realistic soil data, which may be layered. Here, the center line displacement profile of the layered and soft clay are significantly higher than that of the fixed case. The lateral displacement is mainly governed by the soil strength in the uppermost layers. Both the layered soil and soft clay have weaker layers immediately beneath the mudline and are prone to excessive displacement. The values of maximum displacement at the major design levels of the jacket, under various soil conditions, for the sea-state corresponding to

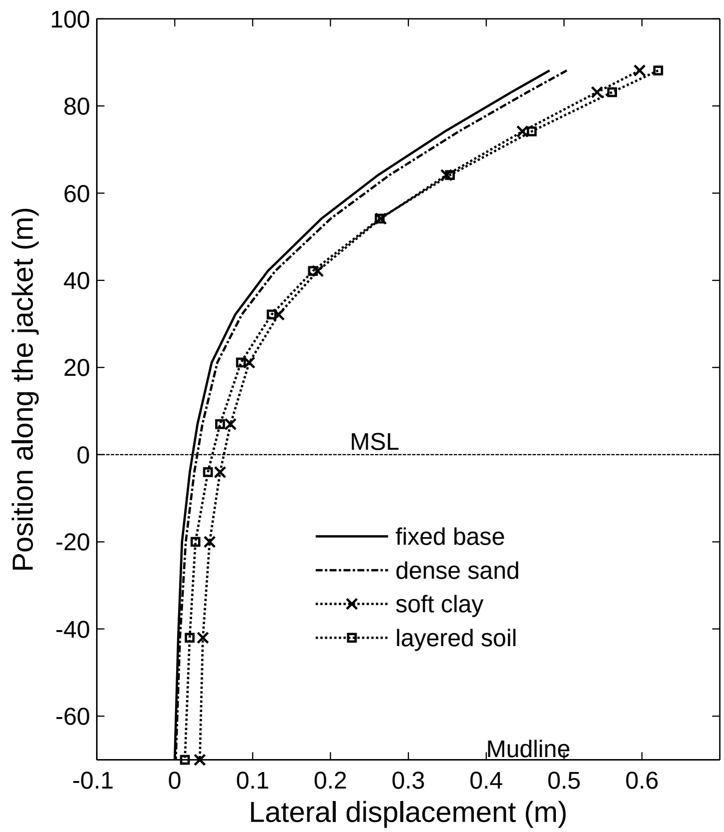

Figure 8: Influence of SSI in OWT analysis

the rated wind speed (Load Case 2, cf. Table 6) are listed in Table 11. Jackets in soft clay and layered soils have tower-top lateral deflections which exceed that of the fixed case by 25% and 30% respectively. Thus, ignoring the influence of SSI could result in underestimation of the lateral displacement profile of the OWT structure.

5.3. Influence of sea-state variation

Here, the impact of environmental loading conditions on the response of the OWT jacket, sited in different soils, is investigated. Winds account for the generation of ocean waves (in addition to swells) and hence, the correlation

Table 11: Displacements along the jacket at rated wind speed

Soil type	Tower top (cm)	Jacket top (cm)	Pile top (cm)
Fixed base	48.0	4.7	0.0
Dense sand	50.3	5.5	0.1
Soft clay	59.7	10.0	3.4
Layered	62.1	8.5	1.4

between them cannot be ignored. Four load cases as defined in Table 6 are analyzed and the results are presented in figures 9, 10 and 11 respectively for dense sand, soft clay and layered soil. Figure 12 is a combination of plots showing the performance of the OWT jacket supported in various soil types, under the effect of different load cases.

The displacement patterns follow a similar trend - lateral displacements increase with increase in wind speed up to the rated wind speed (*i.e* from 6 m/s to 11.4 m/s). Beyond the rated wind speed, there is a reduction is tower displacement, as the wind turbine control systems come into play, limiting the loads at the tower top, for higher wind speeds (Load Case 3 - 24 m/s, cf. Table 6). For extreme winds, above the cut-out wind speed of 25 m/s (*i.e* Load Case 4 - 45 m/s, cf. Table 6), the wind turbine system is shut down (parked rotor) with no power production, so as to prevent failure [44], and this results in moderate tower displacements.

The wave loads on the structure, increase from Load Case 1 to Load Case 4, as shown in Table 6. From Figure 9, it can be noted that the variation of horizontal displacement below the MSL, with increasing wave loads, is nominal, for dense sand, due to its high stiffness values. However, the displacement progressively increases with increasing wave parameters, in the case of soft clay (Figure 10), and to an extend, for layered soil (Figure 11). The relative displacement of the structure, below the MSL, under the influence of wave loads of different magnitudes are clearly visualized in Figure 12. The maxima of displacements along the OWT structure, corresponding to the different cases of

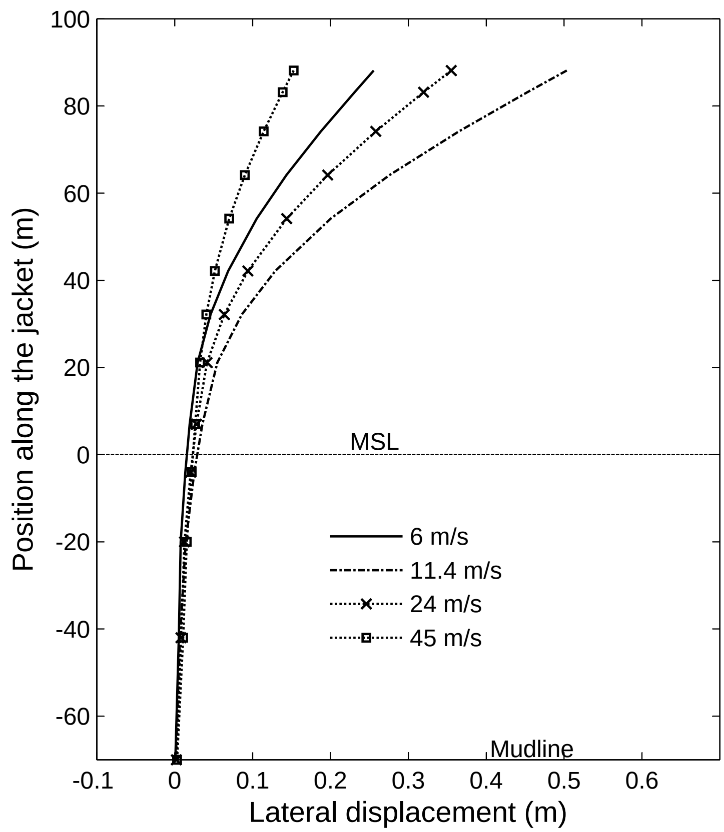

Figure 9: Response variation with sea state - dense sand

environmental loads are detailed out in Table 12. Owing to their reasonably low stiffness values, variations in displacements, of the order of 50% are observed, in the case of soft clay and layered soil, when compared with that of dense sand.

In order to show the variation of the random response with sea states for different stiffness of sand, the ensemble averaged response (tower-top displacement) statistics is shown in Figure 13(a). The ensemble averaged tower-top displacement statistics for different soil profiles is correspondingly shown in Figure 13(b). For layered soil, one can observe very high standard deviation in the response compared to the other soil profiles due to inhomogeneity. Moreover the soil nonlinearity also contributes in making the response non-Gaussian which is

Table 12: Displacements along the jacket for all load cases

Load Case	Tower top (cm)	Jacket top (cm)	Pile top (cm)
Dense sand			
1	25.6	2.9	0.1
2	50.3	5.5	0.1
3	35.5	4.2	0.2
4	15.3	3.3	0.3
Soft clay			
1	28.7	3.9	2.1
2	59.7	9.6	3.4
3	48.3	9.5	5.0
4	18.8	5.9	5.2
Layered soil			
1	39.8	7.6	1.0
2	62.1	8.5	1.4
3	37.0	4.6	1.1
4	27.9	6.3	1.4

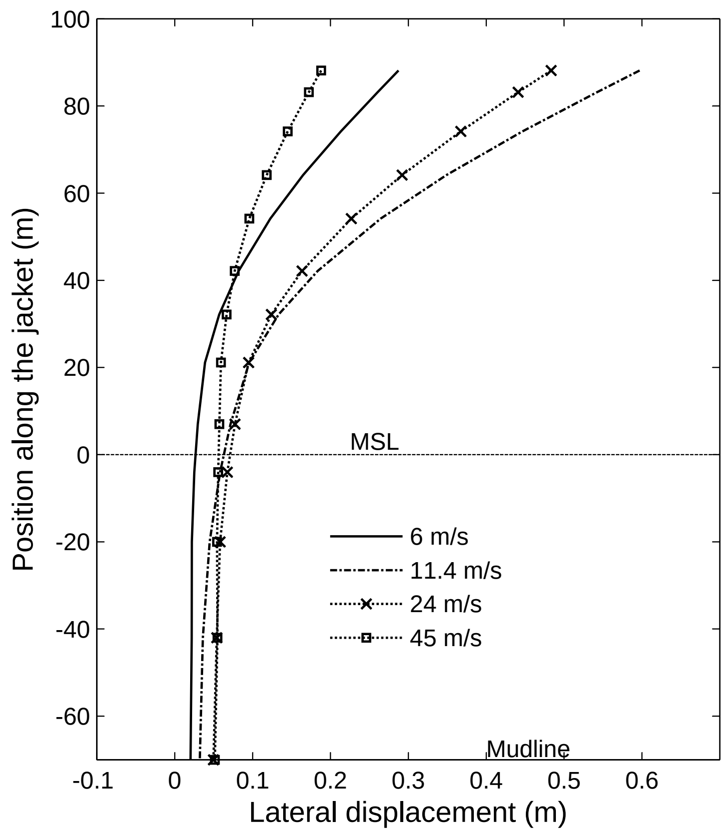

Figure 10: Response variation with sea state - soft clay

amply seen as the averaged kurtosis is less than 3.0 for soil-profiles. Also note that the response is negatively skewed (*i.e.*, mean is less than median) before the rated wind speed and positively skewed (*i.e.*, mean is greater than median) beyond the rated wind speed. This is primarily due to effect of response being controlled after the rated wind speeds to obtain optimum power. Near the rated wind speeds, one observes large displacement compared to the other cases.

5.4. Ultimate strength analysis

Pushover analyses were conducted on the jacket supporting the OWT, for a 100-year survival load case, specified by a sea state of $H_s = 16$ m and $T_p = 18$ s.

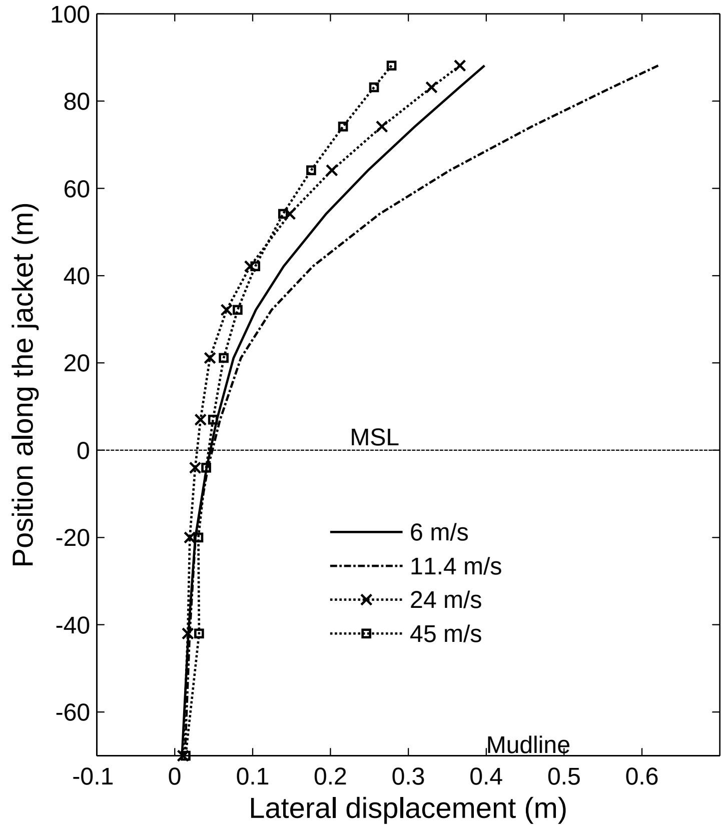

Figure 11: Response variation with sea state - layered soil

Stokes 5−th order wave theory was used for the analysis. Wind load at the hub-height was disregarded. The self weight of the jacket and turbine were initially applied, followed by gradual increment of the wave load to induce global collapse of the jacket. Figure 14 shows the pushover curves for jackets sited in three different soil conditions. Global displacement along the horizontal axis refers to the displacement at the base of the tower. The curves are plotted up to the points of maximum curvature, which are representative of the respective yield strengths. In all three cases, system failure is propagated through failure in the soil - the jacket members do not reach their yield values. Thus, the ultimate strength is simply a function of the soil stiffness.

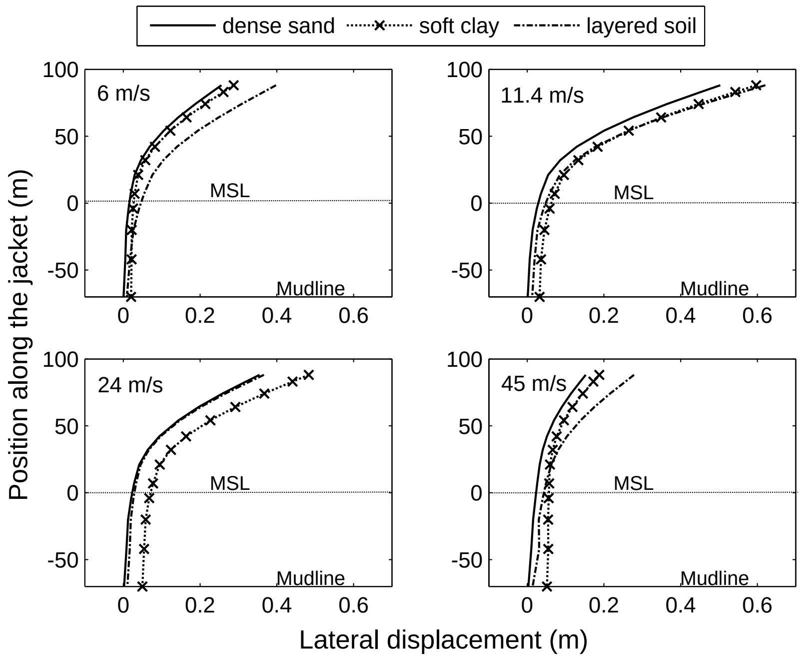

Figure 12: Response variation with sea states and soils

In order to gain a better insight into the mechanics of pile-soil interaction, pushover analyses were done for individual piles embedded in the soils under consideration. The piles are considered to be vertical, with a length of 45m and diameter of 1.8 m. A pile head lateral load of 2 MN was used; this value is representative of the maximum lateral shear at the legs of a fixed jacket during aerodynamic-hydrodynamic analysis in FAST. Piles are pushed to a target pile top displacement of 5% of the diameter $i.e$ 0.09 m and the results are plotted in Figure 15. The softer soils (clay and layered) attains the target displacement at lower load values. However, the pile embedded in dense sand reaches the target displacement only after excessive loading - the response proceeds to the nonlinear regime.

Also, an attempt has been made to study the failure mechanism of piles embedded in varying soil profiles. The target displacement is not considered, in this case and the piles are pushed to failure. The respective displacement

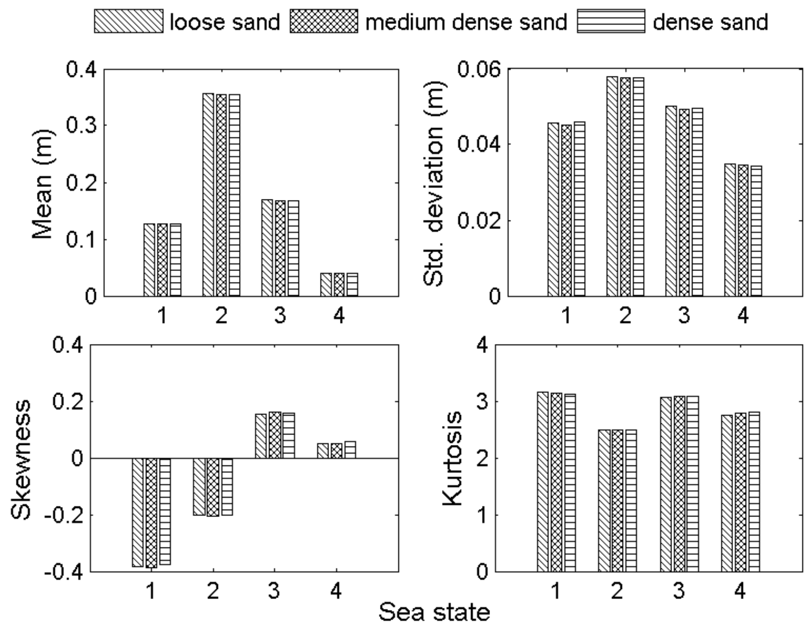

(a) Variation with angle of internal friction for sands

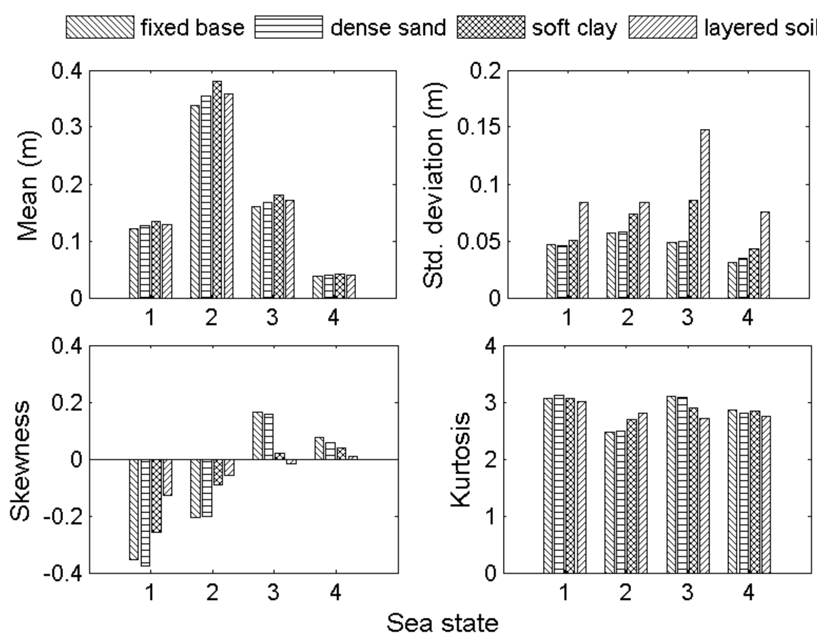

(b) Variation with fixed base and soil profiles

Figure 13: Ensemble statistics for variation of tower top displacement with sea states (For sea state $1-4$ refer Table 6)

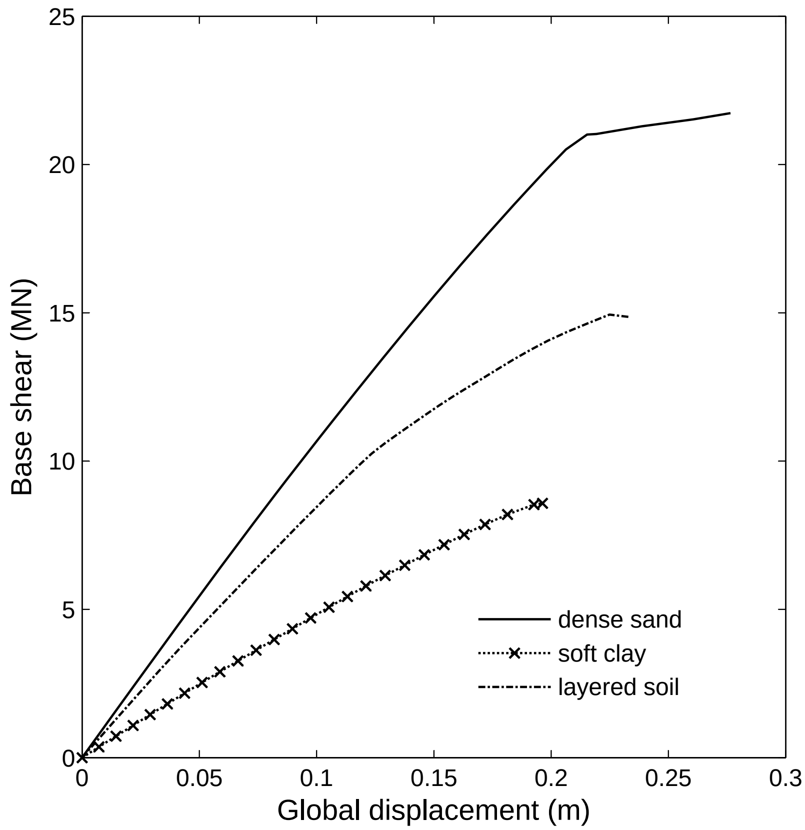

Figure 14: Pushover analysis of OWT jacket

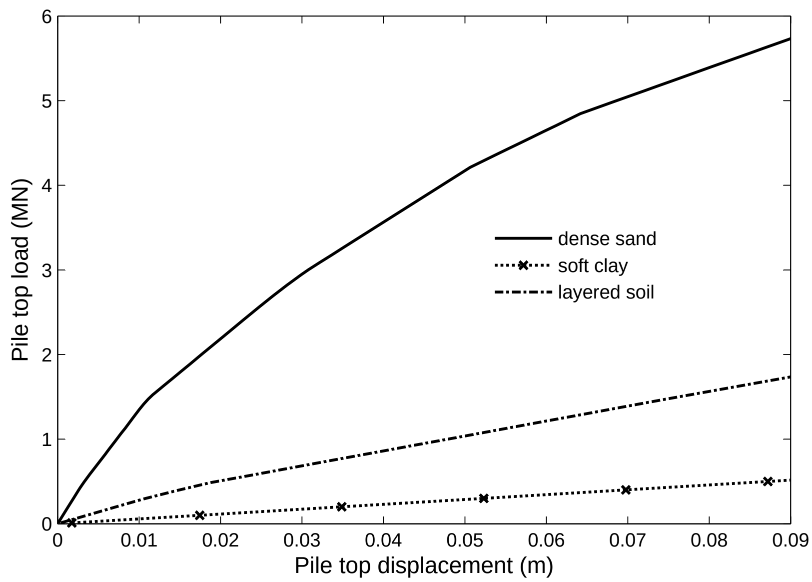

Figure 15: Pushover analysis of only the piles (without the jacket) in different soils

profiles are plotted against depth in Figure 16. The piles behave as flexible ones and failure is induced by bending and formation of plastic hinges in the member. The excessive lateral displacement of the pile in soft clay is due to the lower shear strength and stiffness values in the upper layers.

5.5. Effect of stiffness degradation

The influence of cyclic loading effects on the response of piles supporting the OWT jacket, is investigated, with reference to the dense sand profile. OWTs are subjected to a combination of cyclic and dynamic loads. Cyclic loading on piles can result in stiffness variations in the soil surrounding the pile, leading to accumulation of pile head displacements [65, 16]. The API guidelines attempt to account for cyclic loading, by introducing an empirical factor of 0.9, in the derivation of p-y curves for sand [13]. In the present study, the effects of cyclic loading on piles in sand has been incorporated using the Deterioration of Static p-y curve (DSPY) method [66]. The DSPY method modifies both the soil

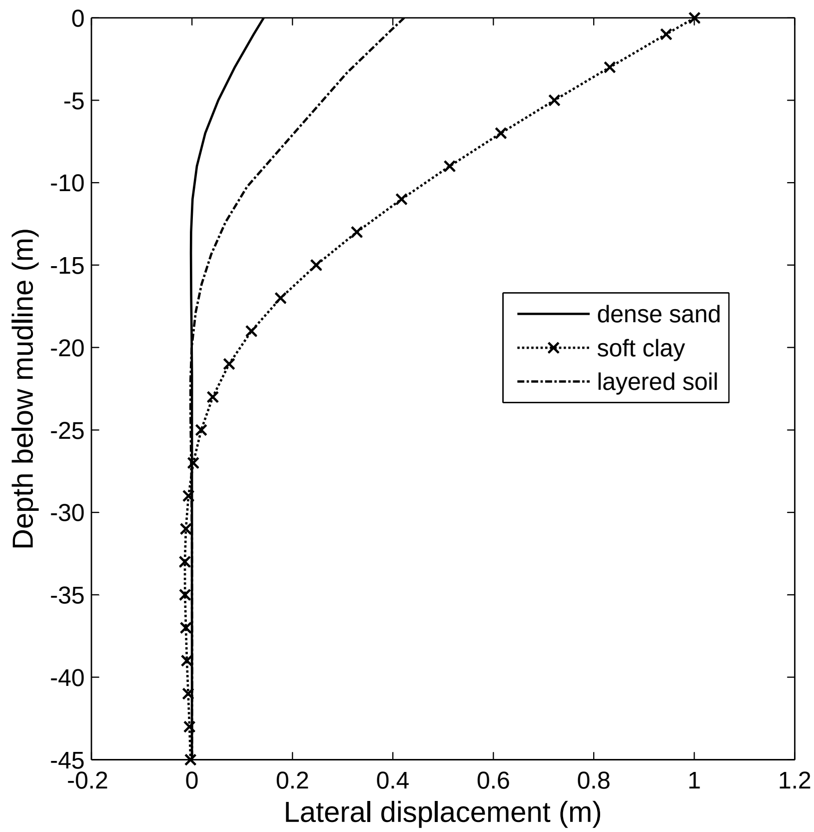

Figure 16: Pile profile at failure

resistance, p and the soil deflection, y of a static nonlinear p-y curve, by taking into consideration, factors such as the type and number of load cycles, density of soil and method of installation of the pile. One-way cyclic loading is assumed as a conservative measure [67] and the piles are considered to be driven into the sandy soil.

Figure 17 shows the variation in the lateral displacement along a pile supporting the jacket OWT in dense sand, with increase in number of load cycles. Extreme wind speed conditions (Load case 4) are considered. Two sets of values are considered for the number of cycles - 100 and 500, and corresponding degraded p-y curves from DSPY are used. The increase in lateral displacement

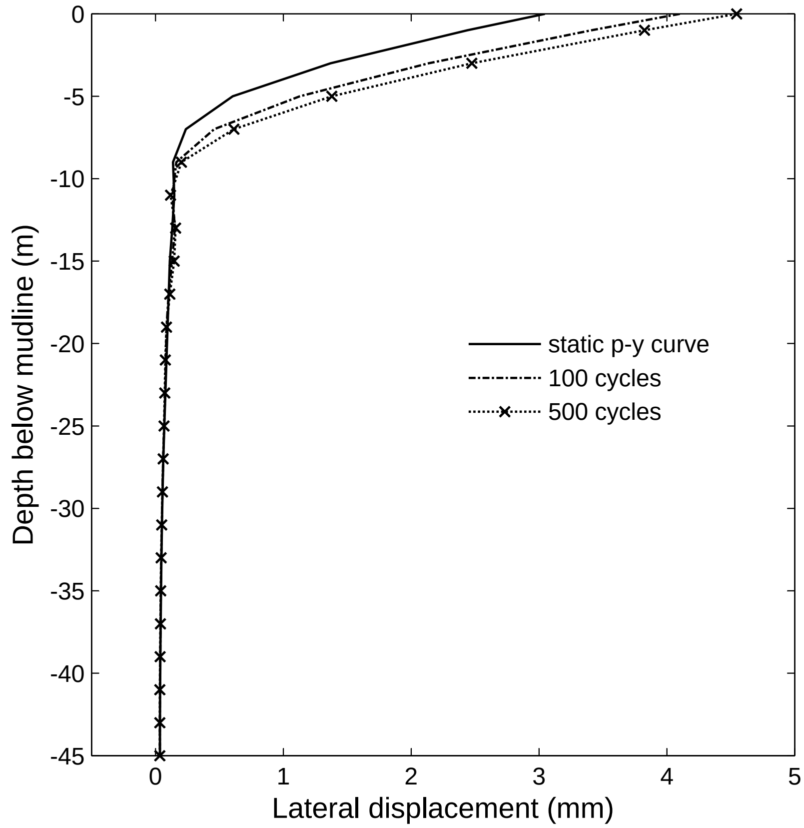

Figure 17: Effect of soil stiffness degradation

with the number of load cycles is confined to the upper layers alone. The pile head displacement for 100 and 500 cycles is greater than that for the static case by 35% and 50% respectively. It may be observed that displacement accumulation takes place at a lower rate, with increase in the number of load cycles, indicating the possibility of consolidation within the soil.

6. Conclusions

Various aspects of soil structure interaction (SSI) in a jacket supporting the NREL 5 MW [26] offshore wind turbine (OWT) has been numerically studied by combining the aerodynamic loads obtained through FAST [28] and hydrodynamic load from USFOS [27]. The jacket is modelled using tubular beam elements and SSI is incorporated in the analysis, through $p-y$, $t-z$ and $Q-z$ curves. The soil profiles are modelled using nonlinear spring-to-ground elements attached to the pile. Three different soil compositions are considered - dense sand, soft clay and a layered profile. Three different wind conditions are studied within operational regime. The wind speeds are so chosen that one is below the rated wind speed ($V_w = 6.0$ m/s), one at rated wind speed ($V_w = 11.4$ m/s) and the last one above the rated wind speed ($V_w = 24$ m/s). Another condition of extreme wind speed ($V_w = 45$ m/s) is studied for idling state of the turbine. The corresponding wave conditions are obtained using JONSWAP spectrum using the relations mentioned in [60]. The turbulent nature of the wind governed by Kaimal spectrum, the irregularity of the waves using JONSWAP spectrum and the soil nonlinearity contribute to the non-linear stochastic/random response. Time domain analyses are performed under these nonlinear random loads. By performing a convergence analysis, it is found that 25 Monte Carlo samples are enough for obtaining the ensemble averaged random response. Since the response is random, ensemble statistics are also reported which also show the non-Gaussian effects due to soil-effects and the applied loads.

One may draw the following conclusions, on the basis of this work:

- including a soil-foundation model induces flexibility into the OWT system, thereby increasing the lateral response. For jackets in soft clay and layered soils, lateral displacements at the tower-top is greater than that of the fixed base (jacket legs pinned to the mudline) configuration by 25 % and 30 % respectively. Such escalated responses can lead to violation of the serviceability limit states.

- when installed in stiff soils (say, dense sand), the behaviour of the jacket-OWT closely follows that of a fixed-based configuration. The variation of the angle of internal friction for uniform sands resulted in marginal variation of lateral response.

- for increasingly severe sea-states, wave loading assumes greater significance, as control effects shut down turbine operations, limiting the load on the tower, but increasing the response below the MSL. For instance, increase in wave heights from (H_s = 2.2 m, T_p = 9.8 s) through to (H_s = 11.1 m, T_p = 13.5 s) brings about a 250% increase in the pile top displacement for soft clay.

- pushover analyses can serve as a means to identify the failure regimen for bottom supported OWTs. In failure, individual piles show flexible behaviour, irrespective of the soil type.

- the effect of stiffness degradation in sandy soils reduces with the increase in the number of load cycles. Pile head displacement after 100 cycles recorded an increase by 35 % over the static case, while that after 500 cycles was 50 %. This reduction is due to possible soil consolidation in the upper layers, with load cycles.

Acknowledgments

The presented work was funded by a research grant from the Ministry of Human Resources, Government of India. The authors are grateful for the financial support. The authors are thankful to Dr Tore Holmas of www.usfos.no and Dr Jason Jonkman of the NREL, for their help with USFOS and FAST, respectively.

References

[1] M. D. Esteban, J. J. Diez, J. S. López, V. Negro, Why offshore wind energy?, Renewable Energy 36 (2) (2011) 444–450. doi:10.1016/j.renene.2010.07.009.

[2] K. Lesny, Foundations for Offshore Wind Turbines: Tools for Planning and Design, VGE-Verlag, 2010.

[3] M. S. Ryu, K. S. Kang, J. S. Lee, A suggestion for the foundation type of offshore wind turbine in the test bed on the basis of economic and constructibility analysis, in: The Twenty-second International Offshore and Polar Engineering Conference, International Society of Offshore and Polar Engineers, 2012, pp. 202–206.

[4] G. Corbetta, I. Pineda, J. Moccia, J. Guillet, The european offshore wind industry–key trends and statistics 2013 (2014).

[5] T. Fischer, W. De Vries, Upwind final report wp 4.1. (wp4: Offshore foundations and support structures), Tech. rep., Upwind (2011).

[6] M. Arshad, B. C. O'Kelly, Offshore wind-turbine structures: a review, Proceedings of the ICE-Energy 166 (4) (2013) 139–152. doi:10.1680/ener.12.00019.

[7] W. Shi, H. Park, J. Han, S. Na, C. Kim, A study on the effect of different modeling parameters on the dynamic response of a jacket-type offshore wind turbine in the Korean southwest sea, Renewable Energy 58 (2013) 50–59. doi:doi:10.1016/j.renene.2013.03.010.

[8] W. Shi, H. Park, C. Chung, J. Baek, Y. Kim, C. Kim, Load analysis and comparison of different jacket foundations, Renewable Energy 54 (2013) 201–210. doi:doi:10.1016/j.renene.2012.08.008.

[9] D. Zwick, M. Muskulus, The simulation error caused by input loading variability in offshore wind turbine structural analysis, Wind energy 18 (8) (2015) 1421–1432. doi:10.1002/we.1767.

[10] S. Voormeeren, P. Valk, B. Nortier, D.-P. Molenaar, D. Rixen, Accurate and efficient modeling of complex offshore wind turbine support structures using augmented superelements, Wind Energy 17 (7) (2014) 1035–1054. doi:10.1002/we.1617.

[11] N. Saha, Z. Gao, T. Moan, A. Naess, Short-term extreme response analysis of a jacket supporting an offshore wind turbine, Wind Energy 17 (1) (2014) 87–104. doi:10.1002/we.1561.

[12] N. Bazeos, G. Hatzigeorgiou, I. Hondros, H. Karamaneas, D. Karabalis, D. Beskos, Static, seismic and stability analyses of a prototype wind turbine steel tower, Engineering structures 24 (8) (2002) 1015–1025. doi:10.1016/S0141-0296(02)00021-4.

[13] API, Recommended practice for planning, designing and constructing fixed offshore platforms–working stress design, API Publishing Services, 2000.

[14] DNV, Offshore Standard-DNV-OS-J101 – Design of Offshore Wind Turbine Structures, Det Norske Veritas AS, 2014.

[15] K. Gavin, D. Igoe, P. Doherty, Piles for offshore wind turbines: a state-of-the-art review, Proc. of the Institution of Civil Engineers - Geotechnical Engineering 164 (GE4) (2011) 245–256. doi:10.1680/geng.2011.164.4.245.

[16] D. Lombardi, S. Bhattacharya, D. M. Wood, Dynamic soil–structure interaction of monopile supported wind turbines in cohesive soil, Soil Dynamics and Earthquake Engineering 49 (2013) 165–180. doi:10.1016/j.soildyn.2013.01.015.

[17] D. Lombardi, S. Bhattacharya, Modal analysis of pile–supported structures during seismic liquefaction, Earthquake Engineering and Structural Dynamics 43 (1) (2014) 119–138.

[18] C. Leblanc, G. Houlsby, B. Byrne, Response of stiff piles in sand to long-term cyclic lateral loading, Geotechnique 60 (GE4) (2010) 79–90.

[19] S. Bhattacharya, S. Adhikari, Experimental validation of soil-structure interaction of offshore wind turbines, Soil Dynamics and Earthquake Engineering 31 (5–6) (2011) 805–816.

[20] S. Adhikari, S. Bhattacharya, Vibrations of wind-turbines considering soil-structure interaction, Wind and Structures 14 (2) (2011) 85–112.

[21] S. Bhattacharya, J. Cox, D. Lombardi, D. Wood, Dynamics of offshore wind turbines supported on two foundations, Proceedings of the ICE - Geotechnical Engineering 166 (2) (2012) 159–169.

[22] S. Bhattacharya, N. Nikitas, J. Garnsey, N. Alexander, J. Cox, D. Lombardi, D. Wood, D. Nash, Observed dynamic soil-structure interaction in scale testing of offshore wind turbine foundations, Soil Dynamics and Earthquake Engineering 54 (2013) 47–60.

[23] W. Shi, H. Park, C. Chung, H. Shin, S. Kim, S. Lee, C. Kim, Soil-structure interaction on the response of jacket- type offshore wind turbine, International Journal of Precision Engineering and Manufacturing - Green Technology 2 (2) (2015) 139–148.

[24] N. Alati, G. Failla, F. Arena, Seismic analysis of offshore wind turbines on bottom-fixed support structures, Philosophical Transactions of Royal Society A 273 (2075) (2015) 20140086.

[25] Y. E. Mostafa, M. H. El Naggar, Response of fixed offshore platforms to wave and current loading including soil-structure interaction, Soil Dynamics and Earthquake Engineering 24 (4) (2004) 357–368.

[26] J. M. Jonkman, S. Butterfield, W. Musial, G. Scott, Definition of a 5-MW reference wind turbine for offshore system development, Tech. Rep. NREL/TP-500-38060, National Renewable Energy Laboratory, Golden, Colorado (2009).

[27] DNV-SESAM, USFOS – Getting Started, Structural Engineering, SINTEF, Marintek (2001).

[28] J. M. Jonkman, M. L. Buhl Jr, FAST – User's guide, Tech. Rep. NREL/EL-500-38230, National Renewable Energy Laboratory, Golden, Colorado (2005).

[29] F. Vorpahl, W. Popko, D. Kaufer, Description of a basic model of the UpWind reference jacket for code comparison in the OC4 project under IEA Wind Annex 30, Fraunhofer Institute for Wind Energy and Energy System Technology IWES.

[30] U. Yukio, S. M. Rashed, The idealized structural unit method and its application to deep girder structures, Computers & structures 18 (2) (1984) 277–293. doi:10.1016/0045-7949(84)90126-3.

[31] T. H. Søreide, J. Amdahl, E. Eberg, T. Holmås, Ø. Hellan, USFOS-A computer program for progressive collapse analysis of steel offshore structures. Theory Manual, SINTEF (1993).

[32] J. Paik, A. K. Thayamballi, A concise introduction to the idealized structural unit method for nonlinear analysis of large plated structures and its application, Thin-walled structures 41 (4) (2003) 329–355. doi:10.1016/S0263-8231(02)00113-1.

[33] B. Skallerud, J. Amdahl, Nonlinear analysis of offshore structures, Research Studies Press, 2002.

[34] T. Moan, Ø. Hellan, M. Emami Azadi, Nonlinear dynamic versus static analysis of jacket systems for ultimate limit state check, in: Proceedings from International Conference on Advances in Marine Structures III, 1997.

[35] M. Emami Azadi, Analysis of static and dynamic pile-soil-jacket interaction behavior, Dr. ing. Thesis, NTNU, Norway.

[36] E. Van Buren, M. Muskulus, Improving pile foundation models for use in bottom-fixed offshore wind turbine applications, Energy Procedia 24 (2012) 363–370. doi:10.1016/j.egypro.2012.06.119.

[37] L. C. Reese, W. F. Van Impe, Single piles and pile groups under lateral loading, CRC Press, 2010.

[38] H. Matlock, Correlation for design of laterally loaded piles in soft clay, in: Offshore Technology Conference, 1970.

[39] H. Song, R. Damiani, A. Robertson, J. Jonkman, A new structural-dynamics module for offshore multimember substructures within the wind turbine computer-aided engineering tool FAST, in: The Twenty-third International Offshore and Polar Engineering Conference, International Society of Offshore and Polar Engineers, 2013, pp. 1–10.

[40] R. Damiani, J. Jonkman, G. Hayman, SubDyn User's Guide and Theory manual, Tech. rep., No. NREL/TP-5000-63062, National Renewable Energy Laboratory, Golden, CO (2015).

[41] B. J. Jonkman, L. Kilcher, TurbSim User's Guide: Version 1.06.00, Tech. Rep. DE-AC36-08-GO28308, National Renewable Energy Laboratory, Golden, Colorado (2012).

[42] P. J. Moriarty, A. C. Hansen, AeroDyn Theory manual, Tech. Rep. NREL/EL-500-36881, National Renewable Energy Laboratory, Golden, Colorado (2005).

[43] J. Van Der Tempel, Design of support structures for offshore wind turbines, TU Delft, Delft University of Technology, 2006.

[44] J. F. Manwell, J. G. McGowan, A. L. Rogers, Wind energy explained: theory, design and application, John Wiley & Sons, 2010.

[45] J. Kaimal, J. Wyngaard, Y. Izumi, O. Coté, Spectral characteristics of surface-layer turbulence, Tech. rep., DTIC Document (1972).

[46] P. S. Veers, Three-dimensional wind simulation, Tech. rep., Sandia National Labs., Albuquerque, NM (USA) (1988).

[47] M. O. Hansen, Aerodynamics of wind turbines, Earth scan, UK, 2008.

[48] S. Chakrabarti, Handbook of Offshore Engineering, Elsevier, 2005.

[49] J. Jia, Essentials of applied dynamic analysis, Springer, 2014.

[50] K. Hasselmann, T. Barnett, E. Bouws, H. Carlson, D. Cartwright, K. Enke, J. Ewing, H. Gienapp, D. Hasselmann, P. Kruseman, Measurements of wind-wave growth and swell decay during the joint north sea wave project (jonswap), Tech. rep., Deutches Hydrographisches Institut (1973).

[51] S. O. Rice, Mathematical analysis of random noise, Bell System Technical Journal 23 (3) (1944) 282–332. doi:10.1002/j.1538-7305.1944.tb00874.x.

[52] S. O. Rice, Mathematical analysis of random noise, Bell System Technical Journal, The 24 (1) (1945) 46–156.

[53] M. Seidel, F. Ostermann, A. Curvers, M. Kühn, D. Kaufer, C. Böker, Validation of offshore load simulations using measurement data from the downvind project, in: Proceedings of European Offshore Wind Conference, Stockholm, Sweden, 2009, pp. 14–16.

[54] Z. Gao, N. Saha, T. Moan, J. Amdahl, Dynamic analysis of offshore fixed wind turbines under wind and wave loads using alternative computer codes, in: Proceedings of the TORQUE 2010 conference, FORTH, Heraklion, Crete, Greece, 2010, pp. 1–9.

[55] M. Zaaijer, Foundation models for the dynamic response of offshore wind turbines, in: Proceedings of Marine Renewable Energy Conference, 2002, pp. 1–8.

[56] E. Bush, L. Manuel, Foundation models for offshore wind turbines, in: ASME Wind Energy Symposium, American Institute of Aeronautics and Astronautics, 2009, pp. 1–7.

[57] M. Seidel, M. Von Mutius, D. Steudel, Design and load calculations for offshore foundations of a 5 MW turbine, in: Conference proceedings DEWEK, German Wind Energy Institute, 2004, pp. 351–356.

[58] M. Mukhopadhyay, D. Choudhury, V. S. Phanikanth, G. R. Reddy, Pushover analysis of piles in stratified soil, in: Proceedings 14th World Conf. on Earthquake Engineering, Vol. 14, International Association for Earthquake Engineering (IAEE) Tokyo, 2008, pp. 1–8.

[59] C. Chen, J. M. Ricles, Analysis of implicit hht-a integration algorithm for real-time hybrid simulation, Earthquake Engineering and Structural Dynamics 41 (5) (2012) 1021–1041. doi:10.1002/eqe.1172.

[60] K. Johannessen, T. S. Meling, S. Haver, Joint distribution for wind and waves in the northern north sea, International Journal of Offshore and Polar Engineering 12 (1) (2002) 1–8.

[61] M. Karimirad, T. Moan, Wave-and wind-induced dynamic response of a spar-type offshore wind turbine, Journal of Waterway, Port, Coastal and Ocean Engineering 138 (1) (2012) 9–20. doi:10.1061/(ASCE)WW.1943-5460.0000087.

[62] R. Mahanta, Pile design for fixed platform for hydrocarbon exploration in indian offshore, in: Proceedings of the Indian Geotechnical Conference, Kochi, Indian Geotechnical Society, 2011, pp. 203–206.

[63] W. Carswell, S. R. Arwade, D. J. DeGroot, M. A. Lackner, Soil–structure reliability of offshore wind turbine monopile foundations, Wind Energy 18 (3) (2015) 483–498. doi:10.1002/we.1710.

[64] W. Dong, Y. Xiang, T. Moan, Time domain modeling and analysis of dynamic gear contact force in a wind turbine gearbox with respect to fatigue assessment, Wind Turbine Technology: Principles and Design (2014) 141.

[65] M. Achmus, Y.-S. Kuo, K. Abdel-Rahman, Behavior of monopile foundations under cyclic lateral load, Computers and Geotechnics 36 (5) (2009) 725–735. doi:10.1016/j.compgeo.2008.12.003.

[66] J. Long, G. Vanneste, Effects of cyclic lateral loads on piles in sand, Journal of Geotechnical Engineering 120 (1) (1994) 225–244. doi:10.1061/(ASCE)0733-9410(1994)120:1(225).

[67] V. D. Krolis, J. Van der Tempel, W. de Vries, Evaluation of foundation design for monopile support structures for offshore wind turbines, in: European Offshore Wind energy Conference, 2007.